

Supporting Information for: Hot Hole Collection and Photoelectrochemical CO₂ Reduction with Plasmonic Au/p-GaN Photocathodes

Joseph S. DuChene^{†§‡}, Giulia Tagliabue^{†§‡}, Alex J. Welch^{†§}, Wen-Hui Cheng^{†§}, and Harry A. Atwater^{†§}*

[†]Thomas J. Watson Laboratory of Applied Physics and [§]Joint Center for Artificial Photosynthesis, California Institute of Technology, Pasadena, California 91125 United States.

[‡]These authors contributed equally to this work.

Methods

Synthesis of plasmonic Au/p-GaN photocathodes

Plasmonic Au/p-GaN photocathodes were constructed via evaporation of Au thin-films onto commercial p-type GaN/sapphire substrates (c-axis 0001 orientation) (5 μm thick GaN) (Pam-Xiamen). Immediately before Au deposition, the p-GaN substrates were first pre-treated with dilute NH₄OH solution (0.02% v/v%) for 30 s to remove native oxide, followed by 30 s of copious washing in Nanopure water. Consistent with previous observations,¹ it was empirically found that such surface treatments were critical for achieving good device performance. The p-GaN/sapphire substrate was then blown dry with N₂ gas and loaded into the vacuum chamber. A 1.5 nm-thick film of Au was then deposited onto the p-GaN surface using electron-beam physical vapor deposition at a base pressure of ca. 1 × 10⁻⁷ torr and a deposition rate of 1.0 Å s⁻¹. The Au/p-GaN films were then annealed in ambient air at 300 °C for 1 h to ensure coalescence of the discontinuous Au thin-film into Au nanoparticles and achieve good adhesion with the underlying p-GaN surface.

Determination of Schottky barrier height at Au/p-GaN interface

Ohmic contacts ($d = 1.5 \text{ mm}^2$) were fabricated via electron-beam physical vapor codeposition of a 10 nm thick Ni/Au (50/50 atomic %) alloy through a shadow mask followed by annealing in ambient air for 1 h at 500 °C. Both Ni and Au targets are deposited simultaneously from two separate sources at a deposition rate of 1.0 Å s⁻¹. A metal-semiconductor Schottky junction was then constructed with 100 nm thick Au contacts ($d = 1.5 \text{ mm}^2$) with electron-beam evaporation through the same shadow mask. Electrical measurements were then conducted under an optical microscope using piezoelectric microcontact probes (Imina

Technologies, miBots™) to electrically address the contact pads on the p-GaN substrate. The current-voltage (I - V) behavior was then collected through a Keithley 236 source-meter unit and operated with custom-built software. The barrier height was determined through fitting of the diode equation to the experimental data.

Synthesis of plasmonic Au/p-NiO photocathodes

Plasmonic Au/p-NiO photocathodes were constructed via evaporation of Au thin-films onto p-type NiO (p-NiO) substrates. The p-NiO films were synthesized on fluorine-doped tin oxide (FTO) glass substrates using electron-beam physical vapor deposition. Ni metal was deposited at a rate of 0.25 \AA s^{-1} under flowing O_2 gas at 6 sccm. After deposition of a 20 nm-thick NiO film on the FTO substrate, a 2 nm-thick film of Au was then deposited onto the p-NiO surface using electron-beam physical vapor deposition at a base pressure of ca. 1×10^{-7} torr and a deposition rate of 1.0 \AA s^{-1} . The Au/p-NiO films were then annealed in ambient air at $300 \text{ }^\circ\text{C}$ for 1 h to ensure coalescence of the discontinuous Au thin-film into Au nanoparticles and achieve good adhesion with the underlying p-NiO surface.

Determination of Ohmic contact at Au/p-NiO interface

Ohmic contacts ($d = 1.5 \text{ mm}^2$) were fabricated via electron-beam physical vapor deposition of a 100 nm thick Ag film through a shadow mask. It has previously been shown that Ag forms Ohmic contacts to p-NiO films.² A 100 nm thick Au contact ($d = 1.5 \text{ mm}^2$) was then constructed with electron-beam physical vapor deposition through the same shadow mask. Electrical measurements were performed under an optical microscope using piezoelectric microcontact probes (Imina Technologies, miBots™) to electrically address the contact pads on the p-NiO substrate. The current-voltage (I - V) behavior was then collected through a Keithley 236 source-meter unit and operated with custom-built software.

Photoelectrochemical characterization of p-GaN and Au/p-GaN photocathodes

All glassware was cleaned with aqua regia (3:1 HCl:HNO₃) before use to remove any trace metal ions. All electrochemical experiments were performed in a three-electrode configuration with the p-GaN or Au/p-GaN photocathode as the working electrode, a Pt wire mesh counter electrode, and a saturated calomel reference electrode all immersed in 50 mM K₂CO₃ (pH 9) electrolyte. The electrolyte was sparged with N₂ gas prior to measurements to remove dissolved O₂ from the solution and experiments were conducted under a N₂ blanket. All electrode potentials were converted to the reversible hydrogen electrode (RHE) scale through the following equation: $E \text{ vs. RHE} = E \text{ vs. SCE} + (0.059 \text{ V pH}^{-1} \times \text{pH}) + 0.2401 \text{ V}$. Electrochemical impedance spectroscopy was performed under dark conditions with a 20 mV sinusoidal amplitude across a range of frequencies (0.1–50 kHz). At higher frequencies (1–10 kHz), the data can be reasonably

represented by a resistor in series with a capacitor.² Open-circuit photovoltage measurements were performed in a quiescent solution after allowing 2-3 hours for Fermi level equilibration between the working electrode and the electrolyte to achieve a steady baseline open-circuit voltage. Incident photon-to-charge conversion efficiency (IPCE) measurements were obtained using a Hg arc lamp (Newport) coupled to a monochromator (slit width 2 mm) to obtain wavelength-dependent photocurrent response. A reference Si photodiode was used to calibrate the light incident on the sample and was then used as reference for power fluctuations during the measurements. All measurements were obtained while the photocathode was potentiostatically poised at $-0.4 V_{\text{RHE}}$ in 50 mM K_2CO_3 electrolyte. The output from the device was fed from the potentiostat into a lock-in amplifier at a chopping frequency of ~ 5 Hz. The IPCE measurements of the Au/p-NiO photocathodes were obtained through a combination of short pass and long pass filters to cover the visible region from 435 nm to 800 nm.

Photoelectrochemical experiments for the plasmon-driven CO_2 reduction reaction

The CO_2 reduction reaction (CO_2RR) was conducted in a three-electrode configuration with Au/p-GaN or bare p-GaN as the working electrode, Pt wire gauze as the counter electrode, and a saturated calomel electrode (SCE) as the reference electrode. All photoelectrochemical experiments were conducted within a custom-built, airtight glass cell equipped with a quartz window. The photoelectrochemical experiments were performed in K_2CO_3 electrolyte (pH 7) that was fully saturated with CO_2 by vigorous bubbling of the cathode and anode compartments for 1 h before commencing with the experiment. The photocathode was potentiostatically poised at $-1.8 V_{\text{RHE}}$ over the course of the experiment. Visible-light irradiation ($\lambda > 495$ nm) was incident on the sample through the quartz window at an incident power of $I_0 = 500 \text{ mW cm}^{-2}$ (measured at the quartz window). Due to the low currents observed from these planar photocathodes, the experiments were performed under sealed “batch reactor” conditions with periodic sampling of the reactor headspace over the course of the reaction with a gas-tight syringe. The gas chromatograph (SRI-8610) was equipped with a Hayesep D column and a Molsieve 5A column using N_2 as carrier gas. The gaseous products were detected using a thermal conductivity detector (TCD) and flame ionization detector (FID) equipped with a methanizer. Quantitative analysis of gaseous products was based on calibration with several gas standards over many orders of magnitude in concentration.

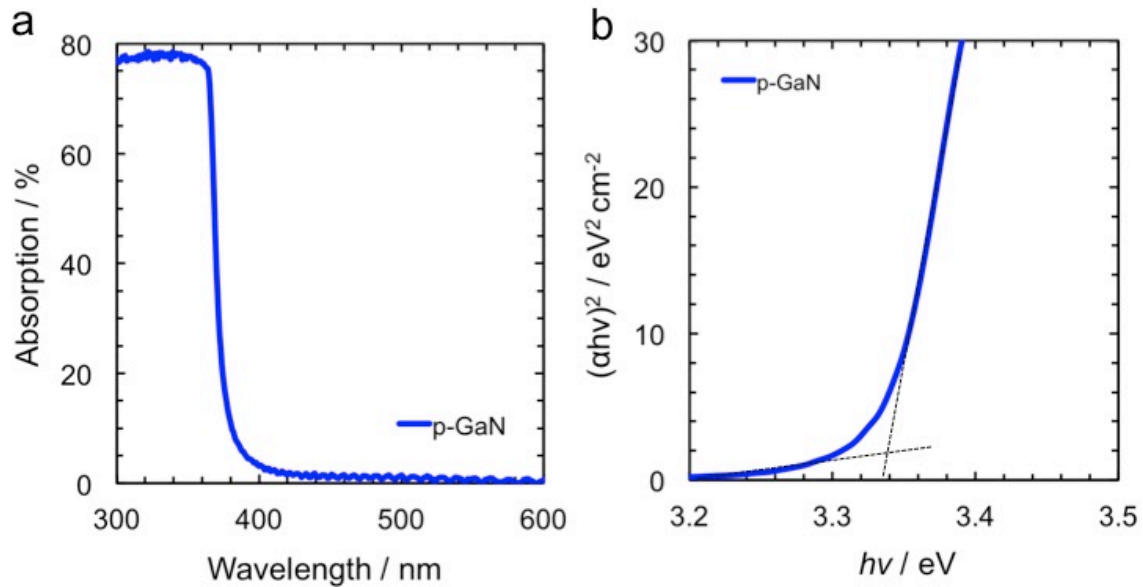


Figure S1. Optical properties of p-type GaN (p-GaN) substrate. (a) Absorption of p-GaN substrate, demonstrating strong absorption in the UV region with no significant features across the visible regime. Thus, any visible-light features observed from the Au/p-GaN system can be attributed to the surface plasmon resonance of the Au nanoparticles. (b) Tauc plot of p-GaN indicates an optical band gap of $E_G = 3.35$ eV, consistent with the expected E_G of 3.4 eV for GaN.³

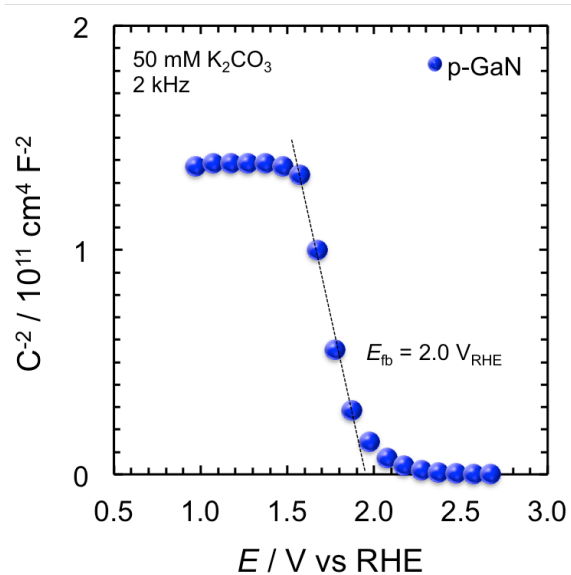


Figure S2. Mott-Schottky plot of electrochemical impedance data obtained from bare p-GaN photocathodes obtained at 2 kHz. The negative slope confirms the p-type character of the GaN substrates used herein. From a linear fit of the data we obtain a carrier concentration of ca. $1 \times 10^{19} \text{ cm}^{-3}$, similar to the acceptor doping level of $N_A = 3\text{--}7 \times 10^{18} \text{ cm}^{-3}$ specified by the manufacturer, and a flat-band potential (E_{fb}) of ca. $2.0 V_{RHE}$ (V vs. RHE).

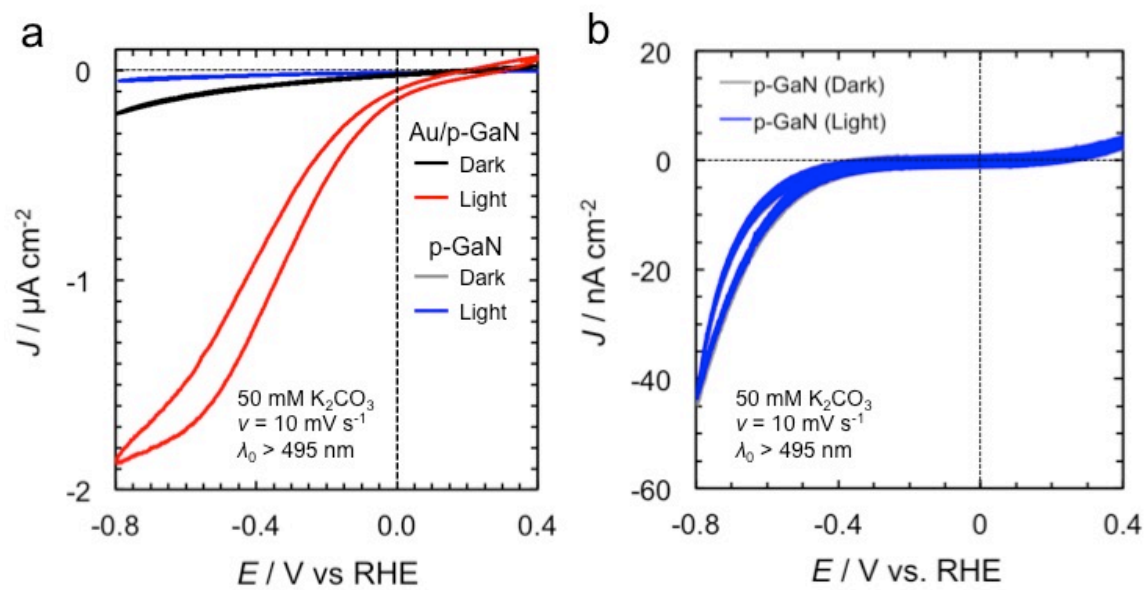


Figure S3. Cyclic voltammetry of photocathodes. (a) Cyclic voltammograms of plasmonic Au/p-GaN and bare p-GaN photocathodes under dark conditions (black and grey curves) and visible-light ($\lambda > 495 \text{ nm}$) irradiation at $I_0 = 500 \text{ mW cm}^{-2}$ (red and blue curves). While the plasmonic Au/p-GaN device exhibits an obvious light response (red curve), no difference in current was observed for the bare p-GaN device (blue curve). (b) Close-up view of the cyclic voltammograms from bare p-GaN photocathode under dark (grey) and visible-light ($\lambda > 495 \text{ nm}$) irradiation (blue) at $I_0 = 500 \text{ mW cm}^{-2}$. No difference could be observed between dark (grey) and light (blue) conditions, as these two curves lay directly on top of one another, confirming that the p-GaN support does not respond to visible light. This observation is consistent with the large band gap of p-GaN (see Figure S1). Therefore, all visible-light responses observed from plasmonic Au/p-GaN photocathodes can be unambiguously assigned to hot-hole injection from Au to the valence band of p-GaN upon plasmon excitation.

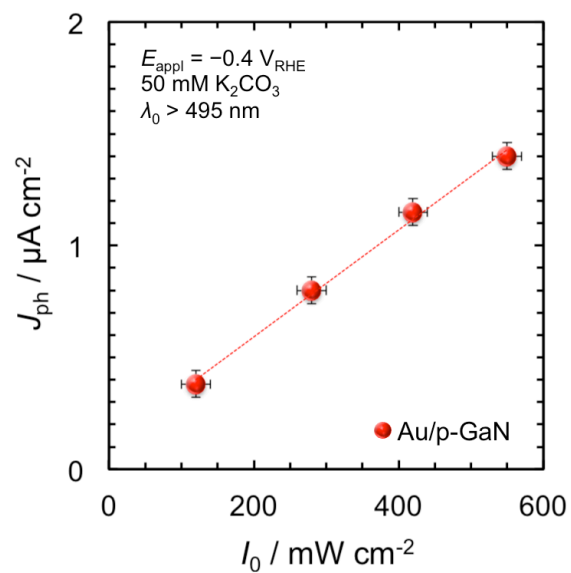


Figure S4. Photocurrent ($J_{\text{ph}} = J_{\text{light}} - J_{\text{dark}}$) response obtained from plasmonic Au/p-GaN photocathodes showing a linear trend with respect to incident light power (I_0).

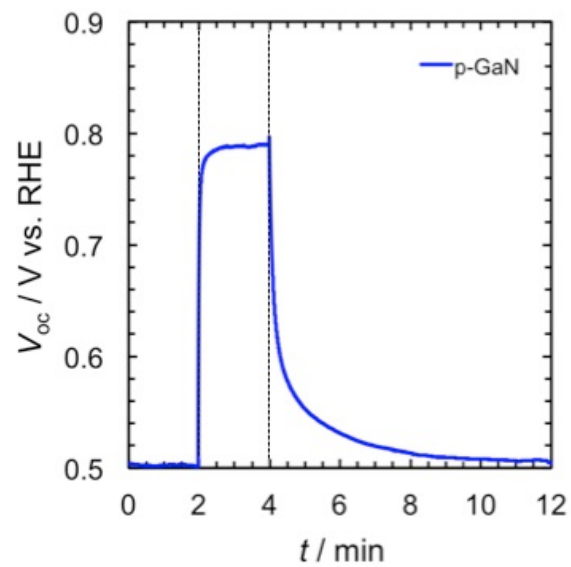


Figure S5. Chronopotentiometry of the open-circuit voltage (V_{oc}) from bare p-GaN photocathodes under UV-light irradiation. The positive shift in V_{oc} upon UV light exposure confirms the p-type character of the GaN substrates used herein.

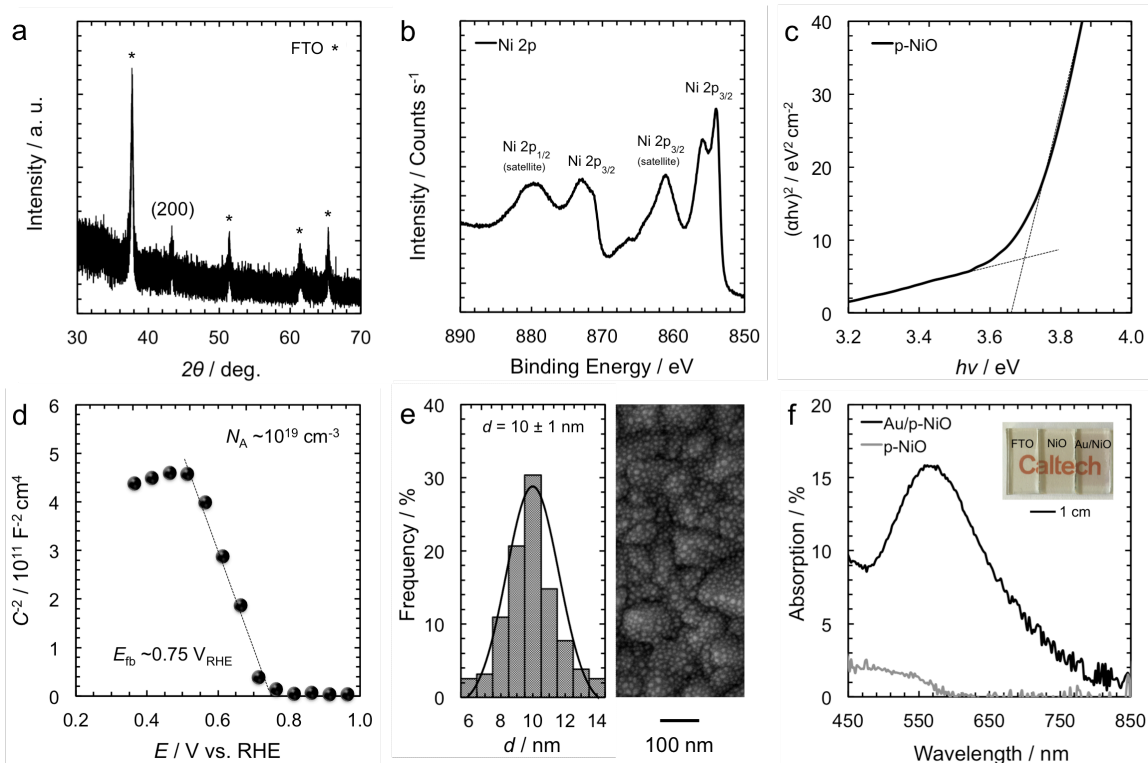


Figure S6. Characterization of p-type NiO films and plasmonic Au/p-NiO films. (a) X-ray diffraction pattern from 20 nm-thick NiO films on FTO glass showing the characteristic (200) peak of NiO. (b) X-ray photoelectron spectroscopy spectrum of the Ni 2p region, showing the characteristic binding energies of NiO. (c) Tauc plot of the NiO film exhibiting a band gap of ca. 3.7 eV. (d) Mott-Schottky plot obtained from 20 nm-thick NiO films on FTO glass substrate, which shows a negative slope indicative of p-type conductivity. From these data, the flat-band potential (E_{fb}) is estimated to be ca. 0.75 V_{RHE} (Volts vs. RHE) with an acceptor concentration of ca. $1 \times 10^{19} \text{ cm}^{-3}$. All these data are consistent with previous literature reports of p-type NiO thin films.² (e) Scanning electron microscopy image of Au nanoparticles uniformly decorated on the p-NiO surface with corresponding size-distribution histogram of the Au nanoparticles, with an average Au diameter of $10 \pm 1 \text{ nm}$. (f) Absorbance of the bare p-NiO photocathode (grey) and the plasmonic Au/p-NiO photocathode (black). A prominent surface plasmon resonance feature due to the Au nanoparticles is observed around 560 nm. Inset shows a digital image of the FTO glass substrate, p-NiO/FTO substrate, and Au/p-NiO/FTO substrate, from left to right. A faint purple color is observed from the Au/p-NiO device.

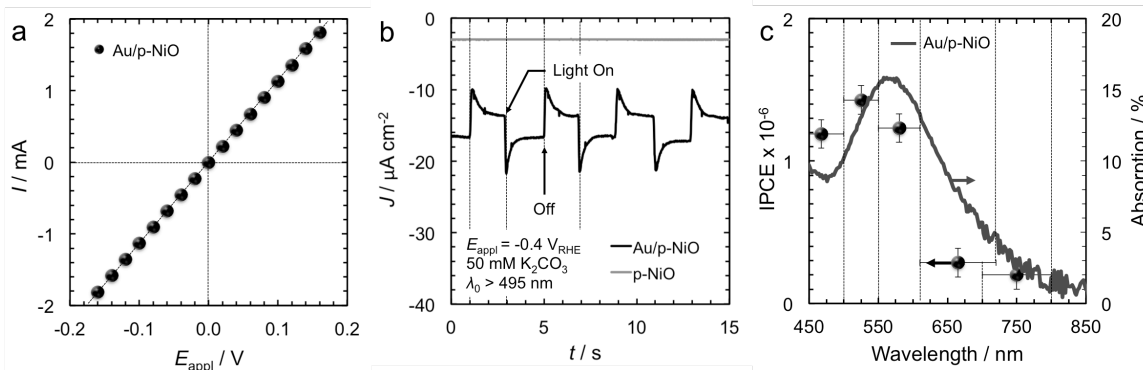


Figure S7. Photoelectrochemistry of plasmonic Au/p-NiO photocathodes. (a) Solid-state current-voltage (I - E_{appl}) behavior from Au/p-NiO films exhibiting Ohmic behavior, consistent with previous literature for Au/NiO contacts. (b) Chronoamperometry from Au/p-NiO photocathodes (black) under visible-light excitation ($\lambda > 495 \text{ nm}$) at 500 mW cm^{-2} while poised at $-0.4 \text{ V}_{\text{RHE}}$. A prompt, reproducible plasmonic photocurrent is clearly observed, indicating hot-hole collection by the p-NiO support upon plasmon excitation. For comparison, the bare p-NiO film (grey) exhibits no observable photocurrent. (c) Photoelectrochemical action spectrum obtained from Au/p-NiO device (black points), showing a clear relationship with the surface plasmon resonance of the Au nanoparticles (black curve).

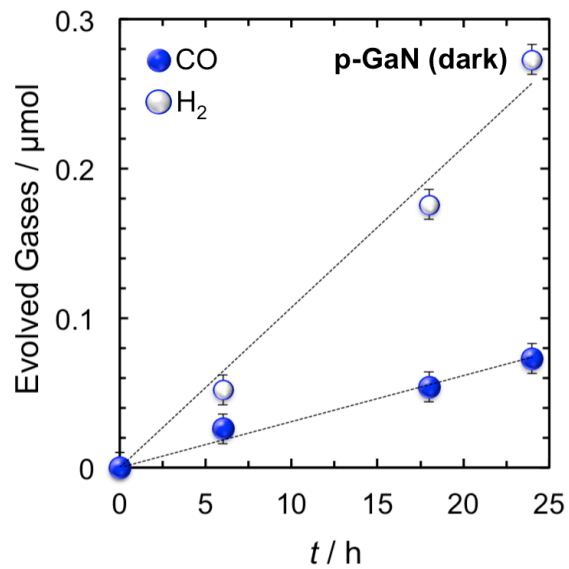


Figure S8. Time-course of gas evolution from bare p-GaN photocathode under dark electrolysis conditions at $-1.8 V_{\text{RHE}}$ in CO_2 -saturated 50 mM K_2CO_3 electrolyte.

Supporting Information References

(1) King, S. W.; Barnak, J. P.; Bremser, M. D.; Tracy, M. C.; Ronning, C.; Davis, R. F.; Nemanich, R. J. *J. Appl. Phys.* **1998**, *84*, 5248-5260.

(2) Thimsen, E.; Martinson, A. B. F.; Elam, J. W.; Pellin, M. J. *J. Phys. Chem. C* **2012**, *116*, 16830-16840.

(3) Kibria, M. G.; Mi, Z. *J. Mater. Chem. A* **2016**, *4*, 2801-2820.